Waveguiding mechanism in tube lattice fibers

Luca Vincetti,[*,1] and Valerio Setti[1]

[1]*Department of Information Engineering, University of Modena and Reggio Emilia, I-41125 Modena Italy*
**luca.vincetti@unimore.it*

Abstract: Waveguiding mechanism and modal characteristics of hollow core fibers consisting of a single or a regular arrangement of dielectric tubes are investigated. These fibers have been recently proposed as low loss, broadband THz waveguides. By starting from a description in terms of coupling between air and dielectric modes in a single tube waveguide, a simple and useful model is proposed and numerically validated. It is able to predict dispersion curves, high and low loss spectral regions, and the conditions to ensure the existence of low loss regions. In addition, it allows a better understanding of the role of the geometrical parameters and of the dielectric refractive index. The model is then applied to improve the tradeoff between low loss and effectively single mode propagation, showing that the best results are obtained with a heptagonal arrangement of the tubes.

OCIS codes: (060.4005) Microstructured fibers; (060.2400) Fiber properties; (260.3909) Infrared, far.

References and links

1. M. Tonouchi, "Cutting-edge terahertz technology," Nat. Photonics **1**(2), 97–105 (2007).
2. M. A. Ordal, L. L. Long, R. J. Bell, S. E. Bell, R. R. Bell, R. W. Alexander, Jr., and C. A. Ward, "Optical properties of the metals Al, Co, Cu, Au, Fe, Pb, Ni, Pd, Pt, Ag, Ti, and W in the infrared and far infrared," Appl. Opt. **22**(7), 1099–20 (1983).
3. M. Naftaly, and R. E. Miles, "Terahertz Time-Domain spectroscopy for Material Characterization," Proc. IEEE **95**(8), 1658–1665 (2007).
4. M. Goto, A. Quema, H. Takahashi, S. Ono, and N. Sarukura, "Teflon photonic crystal fiber as terahertz waveguide," Jpn. J. Appl. Phys. **43**(2B), 317–319 (2004).
5. J. R. Birch, J. D. Dromey, and J. Lesurf, "The optical constants of some common low-loss polymers between 4 and 40 cm^{-1}," Infrared Phys. **21**(4), 225–228 (1981).
6. C. Winnewisser, F. Lewen, and H. Helm, "Transmission characteristics of dichroic filters measured by THz time-domain spectroscopy," Appl. Phys., A Mater. Sci. Process. **66**(6), 593–598 (1998).
7. Y. Jin, G. Kim, and S. Jeon, "Terahertz Dielectric Properties of Polymers," J. Korean Phys. Soc. **49**, 513–517 (2006).
8. G. Gallot, S. P. Jamison, R. W. McGowan, and D. Grischkowsky, "Terahertz waveguides," J. Opt. Soc. Am. B **17**(5), 851–863 (2000).
9. T. Ito, Y. Matsuura, M. Miyagi, H. Minamide, and H. Ito, "Flexible terahertz fiber optics with low bend-induced losses," J. Opt. Soc. Am. B **24**(5), 1230–1235 (2007).
10. R. Mendis, "THz transmission characteristics of dielectric-filled parallel-plate waveguides," J. Appl. Phys. **101**(8), 083115 (2007).
11. K. Wang, and D. M. Mittleman, "Guided propagation of terahertz pulses on metal wires," J. Opt. Soc. Am. B **22**, 2001–2008 (2005).
12. T. Jeon, J. Zhang, and D. Grischkowsky, "THz Sommerfield wave propagation on a single metal wire," Appl. Phys. Lett. **86**(16), 161904 (2005).
13. L. J. Chen, H. W. Chen, T. F. Kao, J. Y. Lu, and C. K. Sun, "Low-loss subwavelength plastic fiber for terahertz waveguiding," Opt. Lett. **31**(3), 308–310 (2006).
14. C. Zhao, M. Wu, D. Fan, and S. Wen, "Field enhancement and power distribution characteristics of subwavelength-diameter terahertz hollow optical fiber," Opt. Commun. **281**(5), 1129–1133 (2008).
15. A. Hassani, A. Dupuis, and M. Skorobogatiy, "Porous polymer fibers for low-loss Terahertz guiding" Opt. Express **16**, 6340–6351 (2008), *http://www.opticsinfobase.org/oe/abstract.cfm?uri=oe-16-9-6340*.
16. S. Atakaramians, S. Afshar Vahid, H. Ebendorff-Heidepriem, M. Nagel, B. Fischer, D. Abbott, and T. Monro, "THz porous fibers: design, fabrication and experimental characterization," Opt. Express **17**, 14053–14062, *http://www.opticsinfobase.org/oe/abstract.cfm?uri=oe-17-16-14053*.
17. F. Benabid, P. J. Roberts, F. Couny, and P. S. Light, "Light and gas confinement in hollow-core photonic crystal fibre based photonic microcells," J. Eur. Opt. Soc. **4**, 09004 (2009).
18. P. Russell, "Photonic-Crystal Fibers," J. Lightwave Technol. **24**(12), 4729–4749 (2006).

#132105 - $15.00 USD Received 10 Aug 2010; revised 6 Oct 2010; accepted 11 Oct 2010; published 19 Oct 2010

19. F. Benabid, "Hollow-core photonic bandgap fibre: new light guidance for new science and technology," Philos. Trans. R. Soc. London, Ser. A. **364**(1849), 3439–3462 (2006).
20. J. C. Knight, J. Broeng, T. A. Birks, and P. S. J. Russell, "Photonic band gap guidance in optical fibers," Science **282**(5393), 1476–1478 (1998).
21. Y. F. Geng, X. L. Tan, P. Wang, and J. Q. Yao, "Transmission loss and dispersion in plastic terahertz photonic band-gap fibers," Appl. Phys. B **91**(2), 333–336 (2008).
22. L. Vincetti, "Hollow core photonic band gap fibre for THz Applications," Microwave Opt. Technol. Lett. **51**(7), 1711–1714 (2009).
23. J. Lu, C. Yu, H. Chang, H. Chen, Y. Li, C. Pan, and C. Sun, "Terahertz air-core microstructure fiber," Appl. Phys. Lett. **92**(6), 64105 (2008).
24. L. Vincetti, "Numerical analysis of plastic hollow core microstructured fiber for Terahertz applications," Opt. Fiber Technol. **15**(4), 398–401 (2009).
25. L. Vincetti, "Single-mode propagation in triangular tube lattice hollow-core terahertz fibers," Opt. Commun. **283**(6), 979–984 (2010).
26. F. Couny, and F. Benabid, "P. J. robets, P. S. Light, and M. G. Raymer, "Generation and Photonic Guidance of Multi-Octave Optical-Frequency Combs," Science **318**, 118–121 (2007).
27. A. Argyros, and J. Pla, "Hollow-core polymer fibres with a kagome lattice: potential for transmission in the infrared," Opt. Express **15**, 7713–7719 (2007), *http://www.opticsinfobase.org/oe/abstract.cfm?uri=oe-15-12-7713*.
28. G. J. Pearce, G. S. Wiederhecker, C. G. Poulton, S. Burger, and P. St. Russell, "Models for guidance in kagome-structured hollow-core photonic crystal fibres," Opt. Express **15**, 12680–12685 (2007), *http://www.opticsinfobase.org/oe/abstract.cfm?uri=oe-15-20-12680*.
29. F. Couny, P. J. Roberts, T. A. Birks, and F. Benabid, "Square-lattice large-pitch hollow-core photonic crystal fiber," Opt. Express **16**, 20626–20636 (2008), *http://www.opticsinfobase.org/oe/abstract.cfm?URI=oe-16-25-20626*.
30. A. Argyros, S. G. Leon-Saval, J. Pla, and A. Docherty, "Antiresonant reflection and inhibited coupling in hollow-core square lattice optical fibres," Opt. Express **16**, 5642–5648 (2008), *http://www.opticsinfobase.org/abstract.cfm?URI=oe-16-8-5642*.
31. C. Lai, B. You, J. Lu, T. Lu, J. Peng, C. Sun, and H. Chang, "Modal characteristics of antiresonant reflecting pipe waveguides for terahertz waveguiding," Opt. Express **18**, 309–322 (2010), *http://www.opticsinfobase.org/abstract.cfm?URI=oe-18-1-309*.
32. M. Kharadly, and J. Lewis, "Properties of dielectric-tube waveguides," Proc. IEE **116**, 214–224 (1969).
33. E. Marcatili, and R. Schmeltzer, "Hollow Metallic and Dielectric Waveguides for Long Distance Optical Transmission and Lasers," Bell Syst. Tech. J. 1783–1809 (1964).
34. S. Selleri, L. Vincetti, A. Cucinotta, and M. Zoboli, "Complex FEM Modal Solver of Optical Waveguides with PML Boundary Conditions," Opt. Quantum Electron. **33**(4/5), 359–371 (2001).
35. L. Vincetti, V. Setti, and M. Zoboli, "Terahertz Tube Lattice Fibers With Octagonal Symmetry," IEEE Photon. Technol. Lett. **22**(13), 972–974 (2010).
36. L. Vincetti, "Confinement losses in honeycomb fibers," IEEE Photon. Technol. Lett. **16**(9), 2048–2050 (2004).
37. L. Vincetti, "Hollow core photonic band gap fiber for THz applications," Microw. Opt. Technol. Lett. **51**(7), 1711–1714 (2009).
38. A. Cucinotta, G. Pelosi, S. Selleri, L. Vincetti, and M. Zoboli, "Perfectly Matched Anisotropic Layers for Optical Waveguides Analysis through the Finite Element Beam Propagation Method," Microw. Opt. Technol. Lett. **23**(2), 67–69 (1999).
39. D. Chen, and H. Chen, "A novel low-loss Terahertz waveguide: Polymer tube," Opt. Express **18**, 3762–3767 (2010), *http://www.opticsinfobase.org/oe/abstract.cfm?uri=oe-18-4-3762*.
40. K. Saitoh, N. A. Mortensen, and M. Koshiba, "Air-core photonic band-gap fibers: the impact of surface modes," Opt. Express **12**, 394–400 (2004), *http://www.opticsinfobase.org/oe/abstract.cfm?URI=OPEX-12-3-394*.
41. P. L. François, and C. Vassallo, "Finite cladding effects in W fibers: a new interpretation of leaky modes," Appl. Opt. **22**(19), 3109–3120 (1983).
42. J. Fini, "Design of solid and microstructure fibers for suppression of higher-order modes," Opt. Express **13**, 3477–3490 (2005), *http://www.opticsinfobase.org/oe/abstract.cfm?URI=oe-13-9-3477*.
43. K. Saitoh, N. Florous, T. Murao, and M. Koshiba, "Design of photonic band gap fibers with suppressed higher-order modes: Towards the development of effectively single mode large hollow-core fiber platforms," Opt. Express **14**, 7342–7352 (2006), *http://www.opticsinfobase.org/abstract.cfm?URI=oe-14-16-7342*.

1. Introduction

Development and enhancement of low loss waveguide covering the electromagnetic spectrum from 300GHz and 30THz, have been driven by a growing interest in Terahertz (THz) technology [1]. In that spectral region, the development of low loss waveguides with high free space coupling efficiency is a tough feature, due to the high conductivity-losses of metals and the high absorption of dielectrics [2–7]. To overcome that problem, several solutions have been proposed borrowing concepts and techniques from both microwaves and photonics technologies [8–16]. All of these try to reduce absorption loss by increasing the percentage of electromagnetic power transmitted through the air.

#132105 - $15.00 USD Received 10 Aug 2010; revised 6 Oct 2010; accepted 11 Oct 2010; published 19 Oct 2010

In optical waveguides, this issue can be addressed with fibers having an air cladding and a subwavelength dielectric core [13] even with one [14] or more [15, 16] air holes. Alternatively, hollow core (HC) fibers confine electromagnetic field inside an air-core surrounded by a microstructured cladding [17–19]. Two techniques can be applied in order to confine the field in a hollow core. The photonic band gap fibers (PBGFs) operate using a cladding with a periodic refractive index which forbids radial propagation at certain frequencies [20]. Low loss region is spectrally limited in the frequency range where the effective index of the mode lies in the photonic bang gap. Numerical analyses have shown transmission bandwidth in the THz range of a couple of hundreds of GHz [21, 22]. In the second technique, fiber cladding does not support photonic band gap [17]. The guided modes confined in the hollow core are prevented from efficiently coupling to cladding due to the weak coupling with cladding modes. Compared to PBGFs, these fibers exhibit much broader low loss regions alternate with high loss regions, and thus they are called broadband HC fibers (BHCFs).

A HC fiber with a cladding formed by a periodic arrangement of Teflon tubes in a triangular lattice (Triangular Tube Lattice - TTL) has been recently demonstrated [23]. Numerical analysis has shown that this fiber falls into the class of the BHCFs [24]. It exhibits very interesting properties such as transmission bandwidth of several hundreds of GHz, low loss, low dispersion and high coupling efficiency with free space propagating beams [24], [25]. Despite that, further improvements are limited by the lack of a proper understanding of waveguiding mechanism and simple models. Interesting and useful models have been proposed for BHCFs with kagome [26–28] and square lattice [29, 30] in visible and near infrared spectral regions. High loss regions correspond to strong resonances between the core modes and particular cladding modes. Since both kagome and square lattice can be seen as an intersection of slab waveguides of infinite width, the resonance frequencies are approximated by the transverse resonance condition [29], corresponding to cut-off frequencies of slab modes. These models are unable to explain some important features of transmission spectrum such as the high loss region at low frequencies and the bandwidth of the high loss regions. These features have been ascribed to the different behavior of TE and TM modes approaching cut-off frequencies [30]. Although the model has been successfully applied to predict high loss regions in square lattice [30] and TTL fibers [24], it requires to introduce an “effective” cut-off conditions for TM modes whose choice is not rigorously defined.

The transverse resonance condition has been also applied to analyzed tube, also called pipe, waveguides for terahertz waveguiding [31]. Fibers with a hollow core surrounded by a thin dielectric layer have already analytically investigated in the 60’s, but focusing only on the modes guided by the dielectric layer [32]. Leaky modes propagating in a hollow core have been analytically analyzed by considering a dielectric with infinite extension [33].

The purpose of this paper is to deepen the knowledge of the guiding mechanism in case of hollow core fibers consisting of a single dielectric tube or whose cladding is composed by a regular arrangement of dielectric tubes, in order to develop a more effective design process. In the tube waveguides, high loss regions are ascribable to the resonance between air core modes and those confined in the surrounding dielectric layer. High loss spectral regions can be accurately predicted by starting from results obtained in [32, 33]. A simple and accurate model for tube lattice fibers, wherein both the core modes and the cladding modes are approximated with those of a single tube waveguide, is presented. Numerical results show that the proposed model is able to predict with high accuracy mode dispersion curves, frequency and spectral width of the high loss regions also in the low frequency region. It is also able to identify the conditions to ensure the existence of low loss spectral regions. The usefulness of the model is then demonstrated by finding out the conditions to improve the tradeoff between propagation loss and effectively single mode operation. The improvements can be obtained just by changing the tube arrangement and the best results are obtained with a heptagonal arrangement of the tubes. The numerical analysis has been performed through a modal solver based on the finite element method (FEM) [34] already successfully applied to

#132105 - $15.00 USD Received 10 Aug 2010; revised 6 Oct 2010; accepted 11 Oct 2010; published 19 Oct 2010

the analysis of loss and dispersion properties of tube lattice fibers [24, 25, 35] as well as photonic band gap ones [36, 37].

The paper is organized as follows. In section 2, the modal solver based on the finite element method used in the numerical analysis is briefly described. In section 3, the single tube waveguide is presented, the properties of its modes are described and the waveguiding mechanism is discussed. In section 4, the model for hollow core fibers with a cladding composed by a regular arrangement of dielectric tubes is presented and it is numerically validated for fiber with hexagonal lattice of tubes. In section 5, the model is applied to improve effectively single mode propagation conditions by considering different tube arrangements. Section 6 contains the conclusions.

2. Numerical analysis method: The finite element method

In order to accurately investigate the properties of the fibers and numerically validate the proposed model, a full-vector modal solver based on finite element method (FEM) has been used. The approach is described in detail in [34] and references therein. Here the most important features are briefly introduced.

The solver is based on the curl-curl equation:

$$\overline{\nabla} \times \left(\hat{p} \overline{\nabla} \times \overline{v} \right) - k_0^2 \hat{q} \overline{v} = 0,$$

obtained by decoupling the Maxwell equations. $\hat{p}$ and $\hat{q}$ represent $\hat{\varepsilon}_r^{-1}$ and $\hat{\mu}_r$ when $\overline{v}$ is the magnetic field $\overline{h}$, and $\hat{\mu}_r^{-1}$ and $\hat{\varepsilon}_r$ when $\overline{v}$ is the electric field $\overline{e}$; $k_0 = 2\pi f / c$ is the wavenumber in the vacuum, being c the light speed in the vacuum and f the frequency.

The expression of the modal solution is $\overline{v} = \overline{V} e^{-\gamma z}$ where $\overline{V}$ is the field distribution on the transverse plane and $\gamma = \alpha + j n_{eff} k_0$ is the complex propagation constant, being α the attenuation constant and n_{eff} the effective index. Applying a variational finite element procedure the following algebraic eigenvalue equation is obtained [34]:

$$\left([A] - \left(\frac{\gamma}{k_0} \right)^2 [B] \right) \{V\} = 0.$$

The eigenvector $\{V\}$ is the discretized field vector, which provides the mode distribution on the transverse plane. The eigenvalue γ allows to evaluate dispersion and loss properties. In particular loss is calculated starting from α, according to

$$LOSS = 20 \log_{10} e \cdot \alpha \cong 8.686 \alpha \ \text{[dB/m]}$$

where α is given in m^{-1}.

In order to enclose the computational domain without affecting the numerical solution, anisotropic perfectly matched layers (PMLs) are placed before the outer boundary [38].

3. Tube waveguide

The cross section of the single tube waveguide is depicted in the left panel of Fig. 1. t, D, and d are, respectively, thickness, inner, and outer diameter of the tube. The tube is made of dielectric material with refractive index *n*. Inside and outside the tube the medium is air with refractive index equal to 1. The analysis of the tube waveguide is very important not only because it has been recently proposed as a simple and low loss THz waveguide [31, 39], but also because, as it will be shown in the next section, the modes of the tube lattice fiber can be obtained directly by the modes of the single tube one.

#132105 - $15.00 USD Received 10 Aug 2010; revised 6 Oct 2010; accepted 11 Oct 2010; published 19 Oct 2010

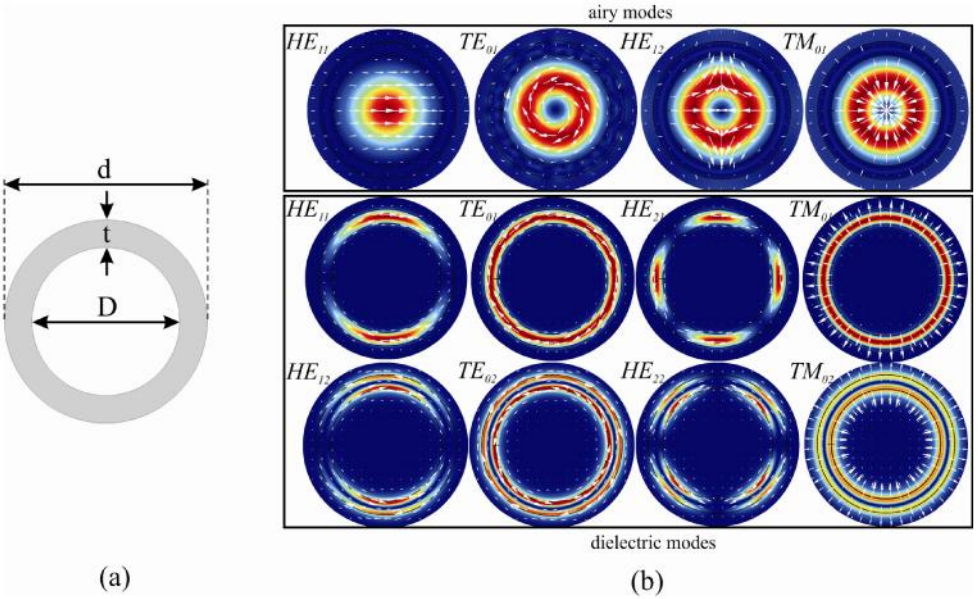

Fig. 1. (a) Transverse section of the tube waveguide. (b) Intensity and electric field distribution of the tube waveguide modes: airy modes (top) and dielectric modes (bottom). The modes are ordered from left to right and, for dielectric modes, from top to bottom following the ordering of their cut-off frequencies.

In the tube waveguide there are two different kind of confined modes: the modes here called "airy" in analogy with kagome lattice fibers [27], whose power is mainly confined inside the air core, and the "dielectric" modes, whose power is mainly located inside the dielectric. Since the effective index of the airy modes is lower than 1 and the tube is surrounded by air, they are leaky. Modal intensity and electric field distributions of the lowest order modes are reported in the right panel of Fig. 1. The first and second subscript μ and ν are, respectively, the numbers of periods in the azimuthal direction and of maxima and minima in the radial direction. The dispersion curves are shown in Fig. 2 in terms of the normalized frequency *F*:

$$F = \frac{2t}{c}\sqrt{n^2 - 1}f. \qquad (1)$$

Dispersion curves of the dielectric modes have been obtained from their characteristics equations [32]. Leakage loss and dispersion curves of the airy modes have been numerically computed. The discontinuities in the dispersion curves of the airy modes are due to the coupling with dielectric modes which causes anti-crossing and high leakage loss. Similar coupling has been observed in hollow core photonic band gap fibers between core and surface modes [40] and in W fibers between core and discrete lossy cladding modes [41]. Since the effective indices of the airy modes are closed to 1, coupling occurs when dielectric modes approach their cut-off frequencies. The normalized cut-off frequencies of the $HE_{1,\nu}$ dielectric modes are $F_c=\nu-1$, and they correspond to the cut-off of the $TE_{\nu-1}$ modes of a slab waveguide with width t or, equivalently, to transverse resonance condition. They have been used to predict high loss regions in kagome [26–28], and square fibers [29,30], and in pipe waveguides [31]. However they cannot explain neither the spectral width of the high loss regions nor the high loss at low frequencies. To overcome this lack, an "effective" cut-off condition for TM slab modes has been introduced to analyze square lattice BHCF [30].

#132105 - $15.00 USD Received 10 Aug 2010; revised 6 Oct 2010; accepted 11 Oct 2010; published 19 Oct 2010

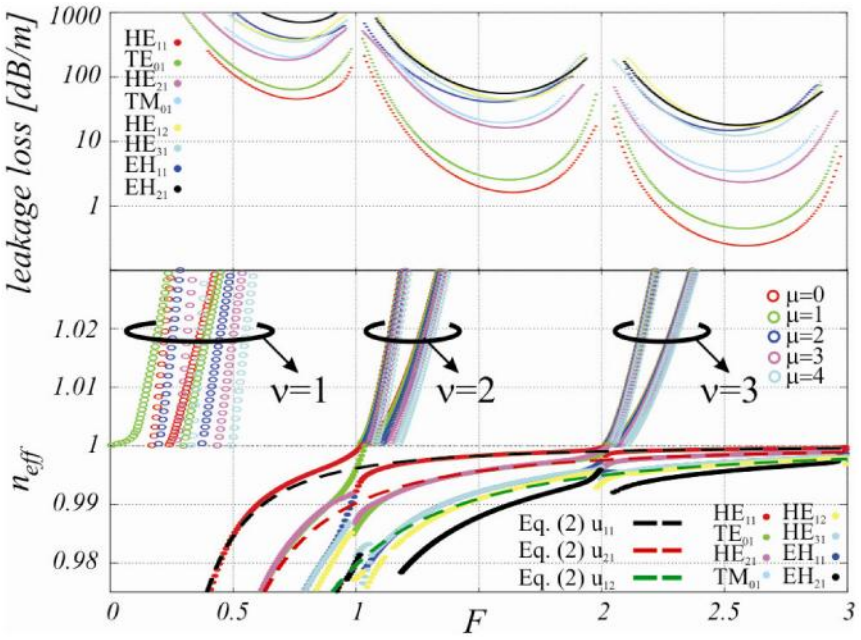

Fig. 2. Loss of the first airy modes (top) and dispersion curves (bottom) of some airy and dielectric modes versus the normalized frequency F. A tube waveguide with n=1.44 and ρ=0.9 is considered. Dashed lines represent the dispersion curves given by Eq. (2).

Figure 2 highlights that, in the tube waveguide, in addition to $HE_{1,\nu}$, there are other dielectric modes with the same radial dependence but higher azimuthal dependence which interact with airy modes. Since their cut-off frequencies are higher, they extend high loss regions. Moreover, cut-off of modes with ν=1 are spread from F=0 to F=0.5 explaining high loss region at low frequency. Actually, for a fixed value of ν, there exist much more dielectric modes with higher azimuthal index μ than those reported in Fig. 2. They have been omitted, because their interaction with airy modes is very weak. In fact, the higher is the azimuthal dependence compared to that of airy modes, the lower is the field overlap and thus the coupling strength [17]. Dielectric mode cut-off can thus be used to estimate high loss spectral width. Cut-off frequencies mainly depend on the ratio ρ between inner and outer tube diameter: $\rho = D/d = 1-2t/d$ [32]. Figure 3 shows the normalized cut-off frequencies of the dielectric modes with low azimuthal dependence versus ρ, for two different values of the dielectric refractive index *n*. As ρ reduces, the cut-off frequencies spread out over a wider range.

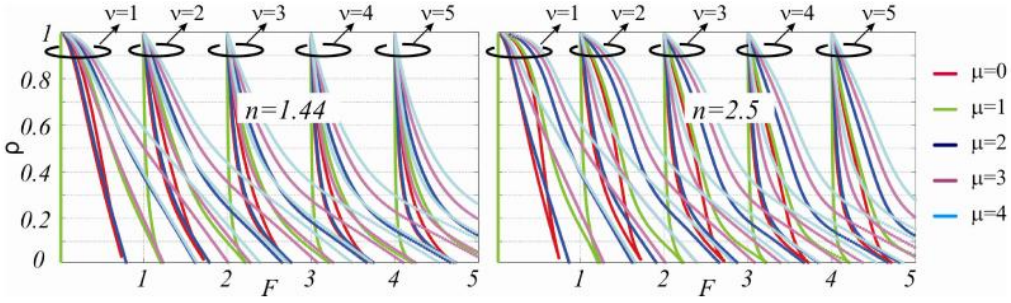

Fig. 3. Normalized cut-off frequencies versus the inner and outer diameter ratio *ρ*, for two different dielectric refractive indices: *n*=1.44, 2.5.

#132105 - $15.00 USD Received 10 Aug 2010; revised 6 Oct 2010; accepted 11 Oct 2010; published 19 Oct 2010

Below a critical value ρ_c, some curves cross each other and there are no more free cut-off spectral regions. Since spreading depends on radial index ν, ρ_c reduces as ν increases. However this value does not significantly depend on the refractive index. On the contrary, for high ρ values, the spreading increases as *n* increases. This means that fibers made of dielectrics with higher refractive index exhibit wider high loss regions. Finally, notice that, the higher the radial index ν and the ratio ρ, the narrower is the high loss region and the better is the approximation of the transverse resonant condition. In [31] ρ varies from 0.875 to 0.947 and *n* between 1.4 and 1.6. Far from resonances, airy and dielectric modes are decoupled. Airy modes are strongly confined inside the HC and their intensities inside the dielectric negligible. This suggests that their characteristics do not significantly depend on cladding parameters. In Fig. 2 dashed lines represent the dispersion curves of the modes of a fiber with an circular air core surrounded by a dielectric with infinite extension obtained from the approximated expression [33]:

$$n_{eff_{\mu\nu}}(f) = 1 - \frac{1}{2}\left(\frac{u_{\mu\nu}c}{\pi 2Rf}\right)^2, \tag{2}$$

being *R* the air core radius, and $u_{\mu\nu}$ is the *ν*–th root of the equation $J_{\mu-1}(u_{\mu\nu}) = 0$. It has been obtained under the assumption that $\pi 2Rf >> u_{\mu\nu}c$. Despite that, the approximation of the airy mode dispersion curves is very good, except at the anti-crossing points.

4. Tube lattice waveguide

Despite the confinement mechanism does not depend on the particular arrangement of the tube lattice, a fiber with triangular tube lattice (TTL) will be initially considered [23, 24]. The cross section is reported in Fig. 4(a). The hollow core is obtained by removing the seven innermost tubes. Since the tubes surrounding the core are centered on the vertices and on the middle points of a hexagon with side length 2*l*, the core shape is approximately a hexagon whose apothem R_1 and circumradius R_2 are:

$$R_1 = d\left(\sqrt{3}\frac{l}{d} - \frac{1}{2}\right), \text{ and } \quad R_2 = d\left(2\frac{l}{d} - \frac{1}{2}\right). \tag{3}$$

The analysis does not depend by the number of tube rings surrounding the core, thus, for sake of simplicity, here a fiber with two tube rings is considered. The guiding mechanism is the same of kagome and square lattice fibers recently developed for visible and near infrared applications [24]. In this kind of fibers the cladding does not exhibit photonic band gap. Cladding modes can be still classified in airy modes and dielectric modes. An example of the two kind of modes is reported in Fig. 5(a). Intensity and electric field distribution of the core modes are reported in Fig. 4(b). The field confinement inside the hollow core is due to the weak coupling between the core modes and the cladding modes [26–30]. Core modes can propagate with low loss if the difference between their effective indices with those of cladding modes is enough high and the field overlap is low. Figure 4(c) shows the propagation characteristics of the first 14 core modes (considering that some modes have a doublet polarization). The leakage loss quickly increases at the resonances with dielectric modes and the dispersion curves are perturbed by the anti-crossing phenomenon. As in the single tube waveguide, this occurs when dielectric modes are closed to the their cut-off frequencies. Far from them, the differences between effective indices of core and dielectric modes are high enough to make low the leakage loss. The irregular spectral behavior of the leakage loss in the low loss regions is due to the weak coupling of the core modes with dielectric modes having high azimuthal dependence whose cut-off fall in this range of frequencies. The High Order Mode (HOM) with the lowest leakage loss is the TE_{01} mode.

Since the core modes are very confined within the core, it is reasonable to think that their dispersion characteristics are similar to those of the airy modes of a tube waveguide. In Fig. 4, the curves obtained through Eq. (2) with core radius $R=(R_1+R_2)/2$ are reported with solid

#132105 - $15.00 USD Received 10 Aug 2010; revised 6 Oct 2010; accepted 11 Oct 2010; published 19 Oct 2010

lines, and they agree very well with the core mode dispersion curves, except around resonances due to anti-crossing.

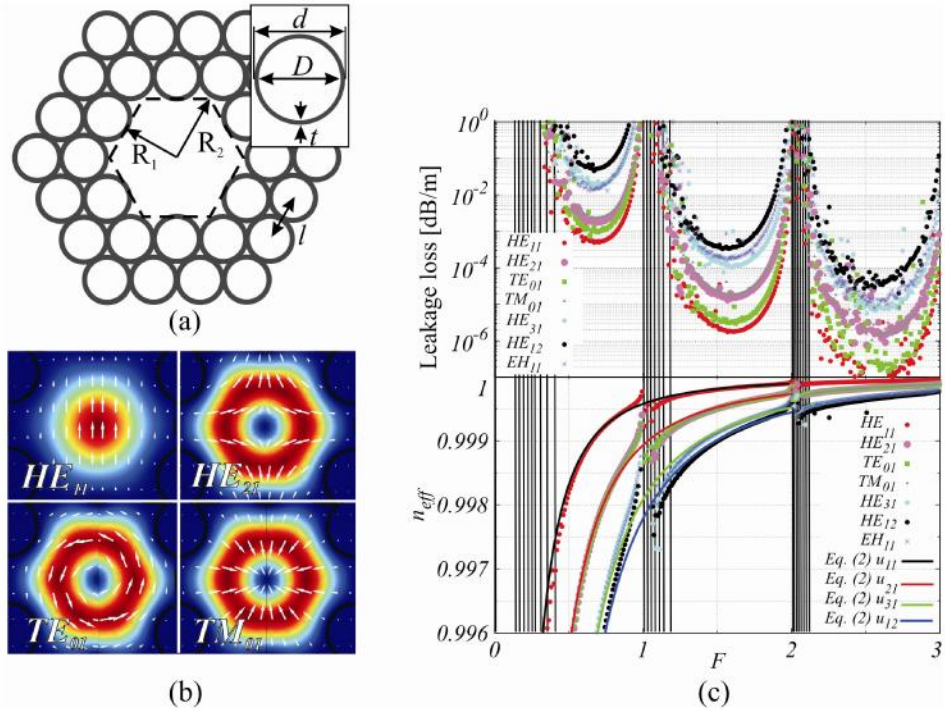

Fig. 4. (a) Transverse section of a TTL fiber. (b) Intensity distribution of the first four core modes. (c) Leakage loss (top) and dispersion curves (bottom) of the first core modes of a TTL fiber with ρ=0.9. Solid lines show curves given by Eq. (2) with $R=(R_1+R_2)/2$ being R_1 and R_2 computed through Eq. (3)

By observing the cladding modes reported in Fig. 5(a), it clearly appears that the field distributions can be seen as composed by multiple replicas of those of a single tube waveguide. This simply observation suggests that the properties of the cladding modes can be obtained from those of a single tube waveguide. The model here proposed follows along the lines of [30]. The cladding of the fiber can be considered as composed by several tube waveguides. By considering them as isolated waveguides and by neglecting any coupling between them, the dispersion curves of the cladding modes can be approximated by those of the modes of the single tube waveguide. This assumption is confirmed by the results reported in Fig. 5(b). On the top, the dispersion curves of the dielectric cladding modes are compared with those of the single tube waveguide around the normalized frequency F=1. Red crosses show dielectric cladding modes with ν=2 and low μ, whereas the green ones show modes with ν=1, 2 and high μ. Squares refer to single tube dielectric modes. Despite the dispersion curve splitting due to the weak coupling between dielectric cladding modes, the agreement is good. The effective indices of the airy cladding modes are reported on the bottom of Fig. 5(b). Red points show effective indices of the HE_{11}-like airy modes. Dashed black line shows Eq. (2) by using the inner radius of the tubes of the cladding R=D/2 and u_{11}. In further confirmation of the assumption, in Fig. 4(c), black solid vertical lines show the cut-off frequencies of the first dielectric modes with ν=1, 2, 3 of the single tube waveguide. They accurately predict high loss regions.

#132105 - $15.00 USD Received 10 Aug 2010; revised 6 Oct 2010; accepted 11 Oct 2010; published 19 Oct 2010

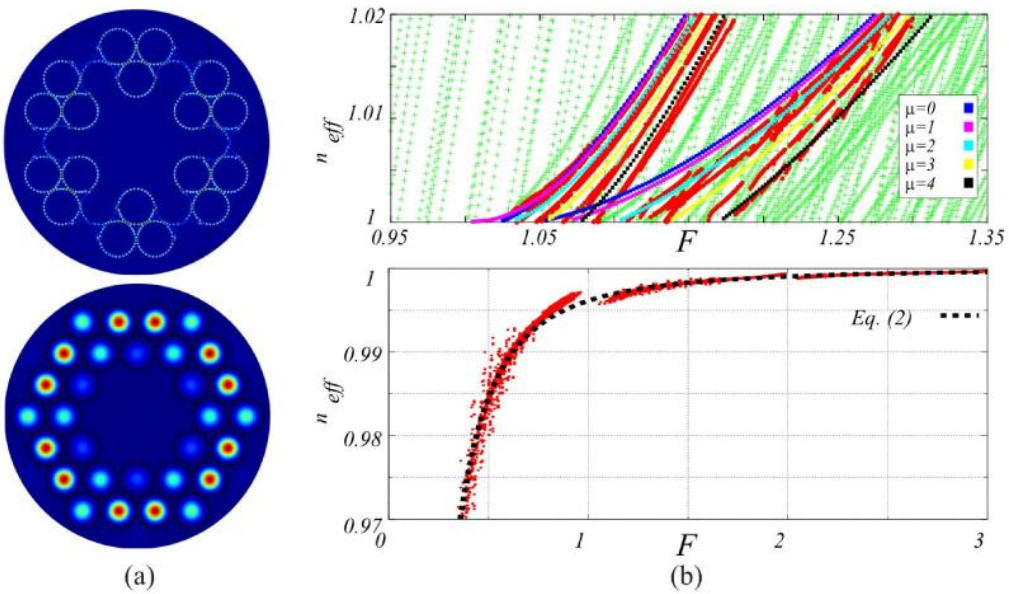

Fig. 5. (a) Intensity distribution of two cladding modes: a dielectric mode (top) and a HE11-like airy mode (bottom). (b) Effective indices of cladding modes versus the normalized frequency F of a TTL fiber with ρ=0.9. Top: dielectric modes around F=1; with high (green crosses) and low (red points) azimuthal dependence; squares show effective index of the dielectric mode of the single tube waveguide analytically computed. Bottom: the airy mode HE_{11}-like (red points); dotted black line shows dispersion curves computed through Eq. (2) with R=D/2.

The effectiveness of the model is then analyzed by varying the geometrical and physical parameters of the fiber. As pointed out in the previous section 3, to have spectral regions free of dielectric mode cut-off frequencies, the ratio ρ must be enough high.

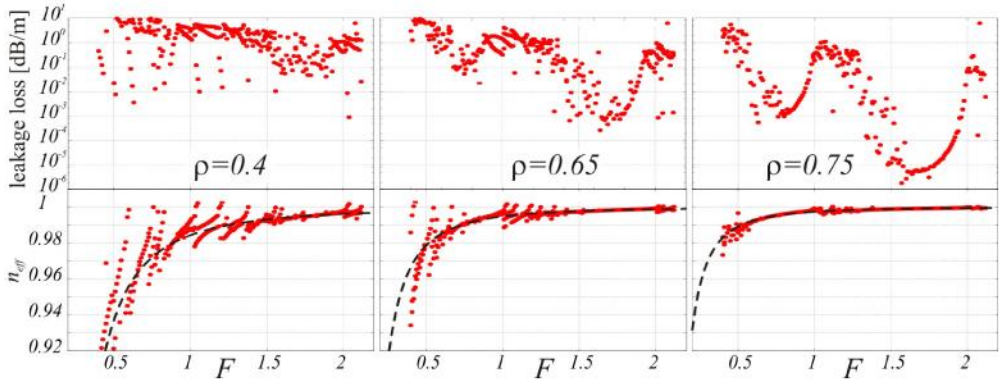

Fig. 6. Leakage loss (top) and dispersion curves (bottom) for n=1.44 and three different values of the ratio ρ: 0.4 (left), 0.65 (middle), and 0.75 (right). Dashed black lines show dispersion curves given by Eq. (2) with u_{11} and $R=(R_1+R_2)/2$ being R_1 and R_2 computed through Eq. (3).

This value is about ρ_c=0.65 and ρ_c=0.45 respectively for the first two low loss regions located between the resonances with modes with ν=1, 2 and with ν=2, 3. In Fig. 6 the leakage loss of the FM is reported for three different values of ρ and n=1.44. According with Fig. 3, with ρ=0.4 there are not low loss regions in the considered normalized frequency range and the dispersion curves exhibit several anti-crossing perturbations due to coupling with dielectric cladding modes. By increasing the ratio to ρ=0.65, a low loss region clearly appears between F=1 and F=2, whereas between F=0 and F=1 the low loss region is only slightly

#132105 - $15.00 USD Received 10 Aug 2010; revised 6 Oct 2010; accepted 11 Oct 2010; published 19 Oct 2010

sketched. Finally, with ρ=0.75 the two low loss regions are clearly depicted and the anti-crossing perturbations concentrated around F=1, and 2. Dispersion curves computed through Eq. (2) and (3) with $R=(R_1+R_2)/2$ are also shown in Fig. 6 with dashed black lines. They are always in good agreement with FM dispersion curves.

Leakage loss and dispersion curves have been also analyzed by varying the refractive index of the cladding tubes. Three different values have been considered: n=1.44, 2.0, and 2.5. Tube thickness and diameters are constant with ρ=0.9. Even in this case, the high loss regions change in agreement with that predicted by Fig. 3. The higher is the refractive index, the wider are the high loss regions and their enlargement is towards the high frequencies. By observing Eq. (1) and (2), normalized frequency depends on refractive index whereas the effective index does not. This is the reason why in Fig. 7, by increasing the refractive index the dispersion curves reduce and the leakage loss increases.

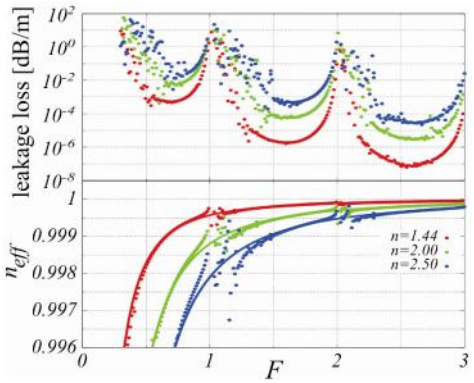

Fig. 7. Leakage loss (top) and dispersion curves (bottom) for ρ=0.9 and three different values of the refractive index n: 1.44 (red), 2.0 (green), and 2.5 (blue). Solid black lines shows dispersion curves computed through Eq. (2) with $R=(R_1+R_2)/2$ being R_1 and R_2 computed through Eq. (3).

Finally, it is important to point out that, since the hypotheses do not depend on the arrangement of the tube, the model can be applied to any kind of tube arrangement. This assumption will be confirmed in the next section.

5. Effectively single mode fiber design

In hollow core fibers, the overlap between mode field and dielectric material plays a key role in determining absorbing loss. This is true especially in THz region due to high dielectric absorption. In order to reduce it, the hollow core size must be significantly larger than the wavelength. Unfortunately this makes the fibers multimode [25]. The multimode propagation can affect the output beam quality, and the signal quality, especially in time domain applications. A way to reduce the detrimental effect of the high order modes is to impair them by increasing the differential loss:

$$\Delta\alpha = \alpha_{FM} - \alpha_{HOM},$$

where α_{FM} is the propagation loss coefficient of the fundamental mode, and α_{HOM} is that of the HOM with the lowest loss. To address this issue, it is possible to reduce the core size at the expense of higher α_{FM} [25]. The purpose of this section is to show that, by using the proposed model, it is possible to improve the tradeoff between $\Delta\alpha$ and α_{FM}, simply by changing the arrangement of the tubes around the core.

#132105 - $15.00 USD Received 10 Aug 2010; revised 6 Oct 2010; accepted 11 Oct 2010; published 19 Oct 2010

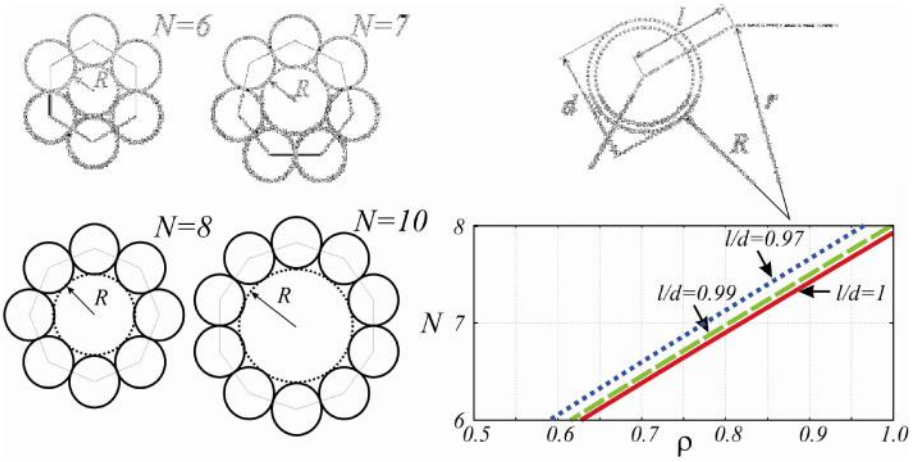

Fig. 8. Left: Fibers geometries obtained by arranging tube on the vertices on a polygon with N sides. Right: on the top detail on the core geometry; on the bottom number N of tubes necessary to guarantee the resonance between core mode TE_{01} and the airy mode HE_{11} versus the ratio diameters ρ, for three different l/d.

A technique to increases the HOM loss without affecting the FM loss is coupling the HOMs with the cladding modes. This technique has been already proposed to obtain effectively single mode operation in solid and hole assisted fibers [42] and in HC-PBG fibers [43]. The coupling was obtained, respectively, by changing the hole spacing between the first and second hole ring or by introducing smaller hole cores around the central one. In the present case, it is not necessary to change cladding structure, because it is possible to directly exploit the airy cladding modes [35]. Furthermore, since their dispersion characteristics are quite similar to those of the core modes (both are well represented by Eq. (2)), phase matching condition is verified over a wide frequency range. The interaction between core and airy cladding modes has been already experimentally observed in [26], and [29], but their role in determining fiber properties has not been thoroughly investigated. Since in THz spectral region the material absorption loss is extremely high, the leakage loss is negligible compared to absorption loss even with just one ring of tubes around the hollow core [25]. This opens up the use of new geometries to arrange the tubes. In particular, as shown in Fig. 8, it is possible to arrange the tubes on the vertices of a polygon with N sides having length l. The relationship between tube diameter d and fiber core radius R depends on N. With some simply geometrical considerations, it is possible to show that:

$$R = \frac{1}{2} d \left(\frac{l}{d} \frac{1}{\sin(\frac{\pi}{N})} - 1 \right). \tag{4}$$

By starting from that observed in the previous sections, the effective index of the core HOM with lowest loss, namely the TE_{01}, can be estimated as:

$$n_{HOM-TE_{01}}(f) = 1 - \frac{1}{2} \left(u_{01} \frac{c}{2\pi R f} \right)^2. \tag{5}$$

Similarly, the effective index of the first airy cladding mode, namely the HE_{11}-like, can be estimated as:

$$n_{Airy-HE_{11}}(f) = 1 - \frac{1}{2} \left(u_{11} \frac{c}{\pi D f} \right)^2. \tag{6}$$

#132105 - $15.00 USD Received 10 Aug 2010; revised 6 Oct 2010; accepted 11 Oct 2010; published 19 Oct 2010

By equating Eq. (5) and (6), replacing Eq. (4), and recalling that $D = d - 2t$, the number N of tubes necessary to guarantee the index matched coupling between core mode TE_{01} and the airy mode HE_{11}–like is:

$$N = \frac{\pi}{\arcsin\left[\frac{l}{d}\frac{u_{11}}{u_{11} + u_{01}\rho}\right]}.$$

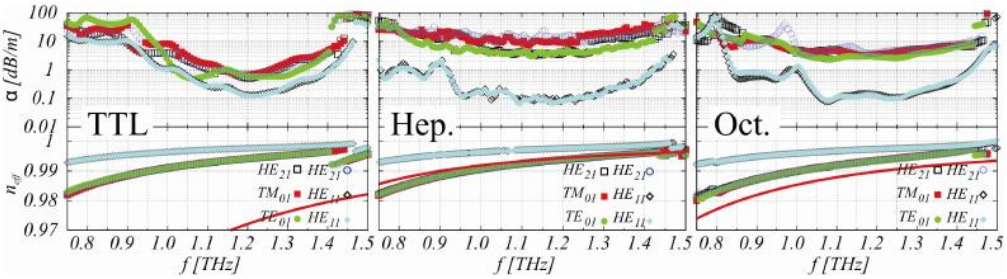

Fig. 9. Leakege loss and dispersion curves for TTL (left), Heptagonal (middle), and Octagonal (right) fibers with a core radius R=1.2*mm* and tube thickness t=0.1*mm*. Solid red lines show dispersion curves of the HE_{11} airy cladding modes.

N versus ρ for three different values of l/d is reported in the right panel of Fig. 8. By excluding values too high and too low of ρ, the best value of N to maximize the coupling is N=7.

To bear out this prediction, three different kind of fibers have been considered: a TTL fiber, a Heptagonal fiber with N=7, and an Octagonal one with N=8. The dielectric material has been assumed to be Teflon, with a refractive index $n=n_r-jn_i$. In the THz spectral region Teflon dispersion is negligible [3–7], so that n_r=1.44 for all the considered frequencies. About imaginary part, several values have been reported in the literature. At f=1*THz*, n_i varies from 0.69E-3, corresponding to about 120*dB/m* [4], to 4.5E-3 corresponding to 870*dB/m* [7]. In the present analysis it has been assumed n_i=1.2E-3 corresponding to 220*dB/m* [5, 6]. By fixing t=0.1*mm*, there is a low loss region centered around 1*THz* and the resonance for ν=2 is at f=1.45*THz*. In the three fibers, the tube diameters have been chosen to have the same core radius R. In order to evaluate only the leakage loss, firstly a lossless material has been considered by assuming n_i=0. In Fig. 9 leakage loss and the dispersion curves of the FM and the first four HOMs for the three kind of fibers are reported in case of R=1.2*mm*. The dispersion curves are approximately the same for the three fibers, according to the theory. Also the minimum of the leakage loss of the FM does not significantly change by changing the fiber. On the contrary, the leakage loss of HOMs significantly increases passing from TTL to Octagonal and, finally, to Heptagonal fiber, according to the theory. In the Heptagonal fiber, the improvement is about a order of magnitude if compared to TTL one. In fact, as shown in Fig. 9, in the Heptagonal fiber, the dispersion curve of the cladding airy mode HE_{11}–like (solid red line) is much closer to those of HOMs than in the other fibers. Furthermore this phase matching condition is maintained over a broad range. In order to show more clearly the improvement, the differential loss $\Delta\alpha$ versus the minimum of the FM loss α_{FM} for different core radius is shown in Fig. 10 by considering n_i=0 and n_i=1.2E-3. All fibers exhibit a quasi-linear relationship. The Heptagonal fiber exhibits the sharpest curves in case of both lossless and lossy medium. As the core size increases, ρ tends to 1, because d increases and t is constant to 0.1 mm. By observing Fig. 8, this means that the optimum value of N changes from 7 to 8. This is why, with R=1.6 *mm*, the values of the Octagonal and the Heptagonal fibers are the same.

#132105 - $15.00 USD Received 10 Aug 2010; revised 6 Oct 2010; accepted 11 Oct 2010; published 19 Oct 2010

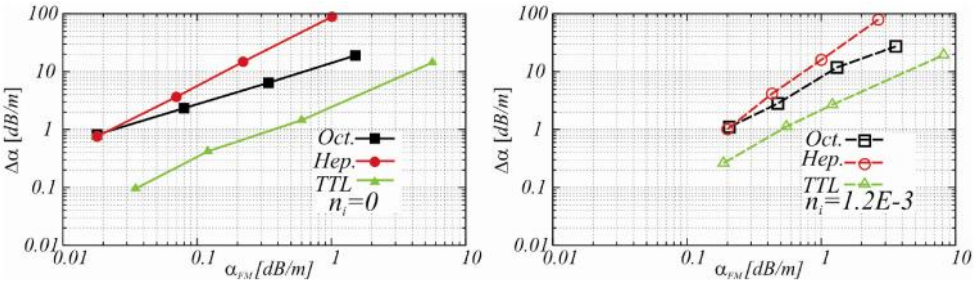

Fig. 10. Differential loss versus the minimum of the FM loss for different core radius in case of lossless dielectric (left) and lossy dielectric (right) with n_i=1.2E-3. By starting form bottom-left side the core radii are: R=1.6*mm*, 1.2*mm*, 0.97*mm*, 0.73*mm*.

The material absorption shifts the curves toward higher FM loss. In this case, loss is composed by leakage and absorption loss. The effect of material absorption on the total loss is different for the different fibers: the lower is the leakage loss, the higher is the sensitivity towards material absorption, whereas the larger is the core, the lower is the sensitivity. In the Heptagonal fiber, absorption increases the FM loss, whereas the differential loss is substantially unchanged. In the Octagonal fiber, the differential loss is unchanged only for large core. Finally, in TTL fibers the absorption effects on the FM loss and on the differential loss are comparable. Although the threshold over which the fiber can be considered effectively single mode depends on the particular application, to fix the ideas, let assuming a differential loss of 20 *dB/m*. Figure 10 shows that with TTL fiber a core of 0.73 *mm* is required, and the FM loss is about 8 *dB/m*. The same condition is obtained with a core around of 1 *mm* and a FM loss of 1 *dB/m* in case of Heptagonal fiber, that is almost a decade lower than TTL one.

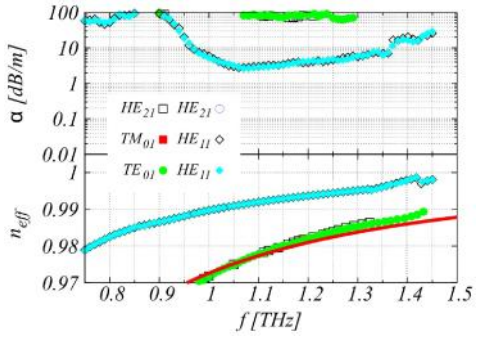

Fig. 11. Leakege loss and dispersion curves of a heptagonal fiber with a core radius R=0.73*mm* and tube thickness t=0.1*mm*. Solid red lines show dispersion curves of the HE_{11}-like airy cladding modes.

Finally, in order to show that effectively single mode operation can be obtained over a broadband, Fig. 11 shows loss and dispersion characteristics versus the frequency of a Heptagonal fiber with R=0.73 *mm*, cladding tubes with diameter d=1.18 *mm* and thickness t=0.1 *mm*. The differential loss is always higher than 70 *dB/m*, whereas the FM loss is lower 10 *dB/m* over a band 400 *GHz* with a minimum of 2.8 dB/m at 1.07 *THz*.

6. Conclusion

In this paper the waveguiding mechanism in hollow core fibers composed by a single dielectric tube or a regular arrangement of tubes has been thoroughly analyzed. The high loss regions are due to the resonant coupling between core modes and dielectric modes like in the kagome and square BHCFs.

#132105 - $15.00 USD Received 10 Aug 2010; revised 6 Oct 2010; accepted 11 Oct 2010; published 19 Oct 2010

In the single tube waveguides, the high loss spectral regions and the dispersion curves of the core modes can be accurately predicted by starting from analytical equations. In the tube lattice fibers, a simple and useful model has been proposed. In the model, both the core and the cladding modes are described in terms of the modes of a single tube waveguide. Numerical results show that the model is able to predict loss and dispersion properties with the change of geometrical and physical parameters, allowing a better understanding of the role of tube diameter, thickness, and refractive index into design process. High loss regions mainly depend on ratio between inner and outer tube diameters, whereas the dielectric refractive index dependence is weaker. The model has been then applied to improve effectively single mode operation of the fiber by enhancing the coupling between high order core modes and airy cladding modes. It has been analytically shown, and then numerically verified, that fibers made of tubes arranged in a heptagonal symmetry exhibit the best tradeoff between high HOMs loss and low FM loss.

Finally, since there is a similarity between a circle and a hexagon, it is possible that the proposed model could be also applied to the analysis of BHCFs with a kagome lattice. These aspects will be subject of future investigations.

#132105 - $15.00 USD Received 10 Aug 2010; revised 6 Oct 2010; accepted 11 Oct 2010; published 19 Oct 2010